

# Modeling the LAGO's detectors response to secondary particles at ground level from the Antarctic to Mexico

R. Calderón-Ardila, A. Jaimes-Motta, J. Peña-Rodríguez, C. Sarmiento-Cano,  
M. Suárez-Durán and A. Vásquez-Ramírez

for the LAGO Collaboration





# The Latin American Giant Observatory (LAGO)

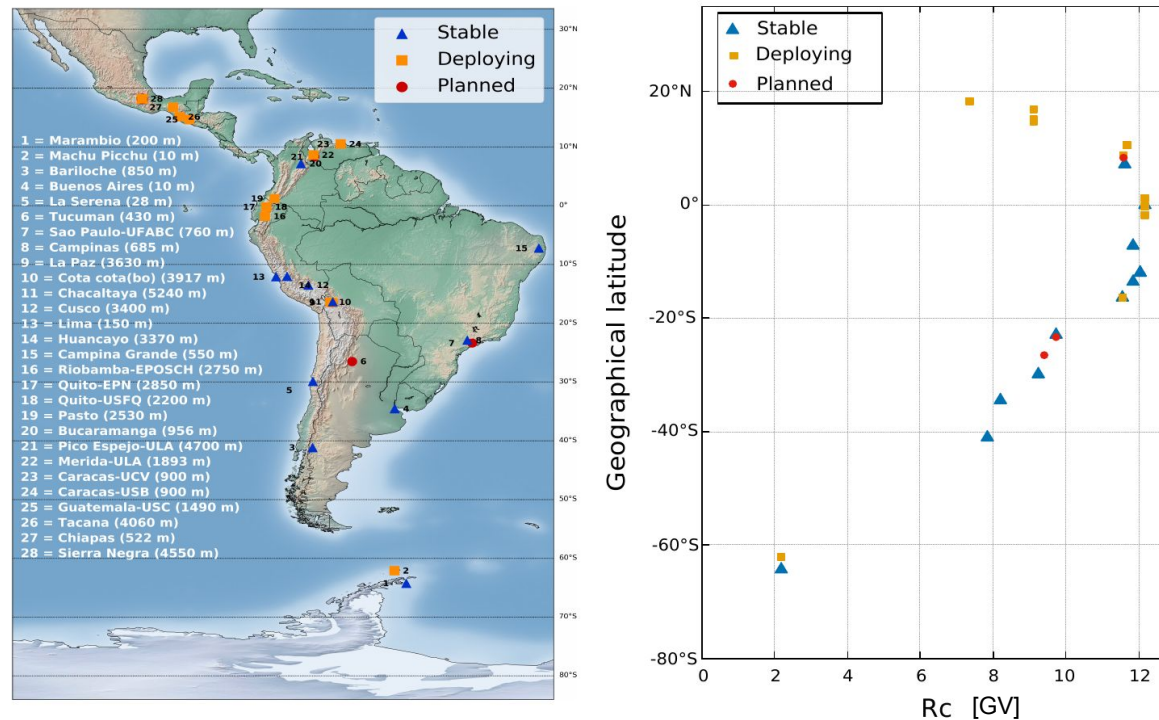
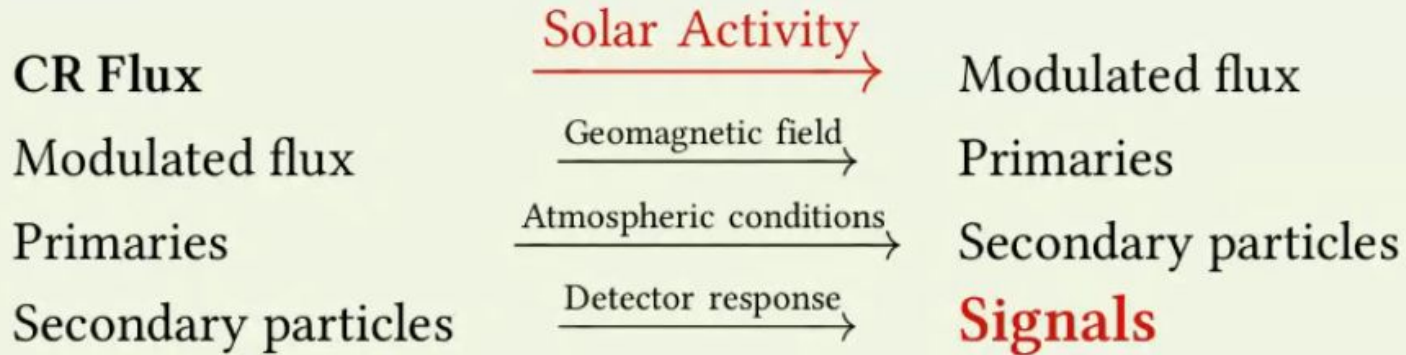


Figure 1: (Left) Geographical distribution and altitudes of the Latin American Giant Observatory water Cherenkov detectors [1]. The ones in operation are represented with blue triangles, orange squares are used for those in deployment and the planned sites are indicated in red circles. (Right) Vertical rigidity cutoff at each LAGO site.

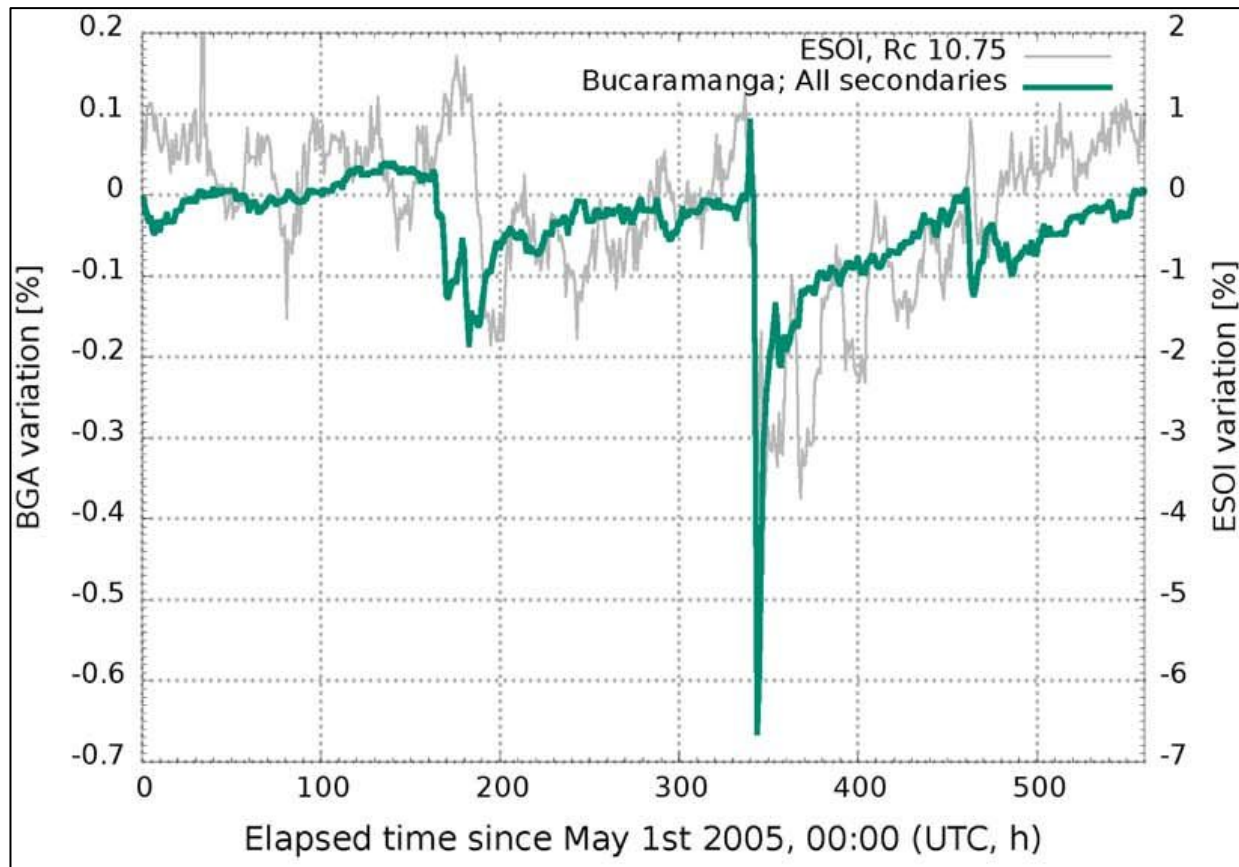
# The LAGO Space Weather Program

## Connections



## Synergy

Flux variation of signals at detector level  $\Leftrightarrow$  Solar Activity



Asorey, H., Núñez, L. A., Suárez-Durán, M. Preliminary results from the latin american giant observatory space weather simulation chain. *Space Weather*

# Secondary flux simulation with ARTI

## Detailed simulation chain

- Directional rigidity cut-off at each site  $R(\varphi, \lambda, \theta, \phi)$ :
  - ◆ Corrected magnetic field with the IGRF model (up to 5 earth radius) and Tsyganenko 2001 (more than 5 earth radius)
- Primary flux at the top of the atmosphere (CORSIKA(112km)\* simulations for each site  $(\varphi, \lambda, h)$ ):
  - ◆ Measured spectra for all nuclei  $1 \leq Z_p \leq 26, 1 \leq A_p \leq 56$
  - ◆  $(R(\theta, \phi) \times Z_p) \leq (E_p/GeV) \leq 10^6, 0^\circ \leq \theta \leq 90^\circ$
  - ◆ Integrated primary flux:  $\sim 10^7 - 10^8 \text{ hour}^{-1} \text{m}^{-2} (\geq 5 \text{ hours at each site})$
- Secondary flux at detector level
- Detector response:
  - ◆ Detailed GEANT4 model

\* Corsika version 76500

# Estimation of Cosmic Background Radiation at the Ground Level

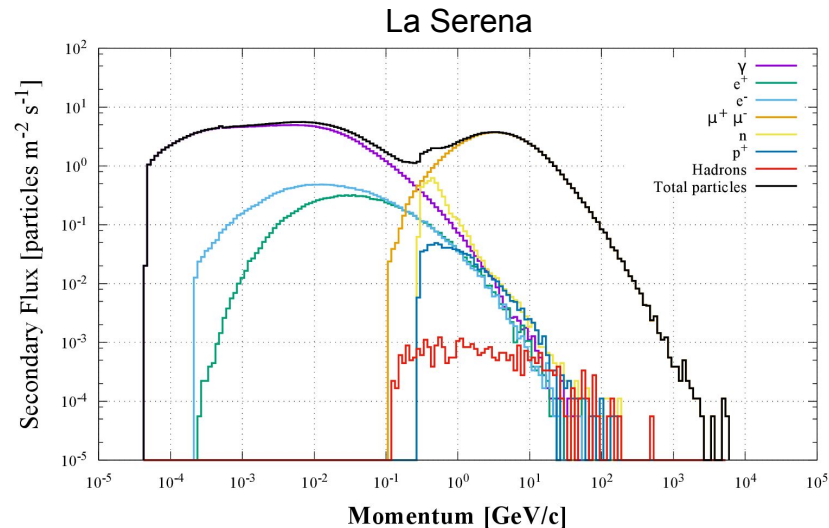
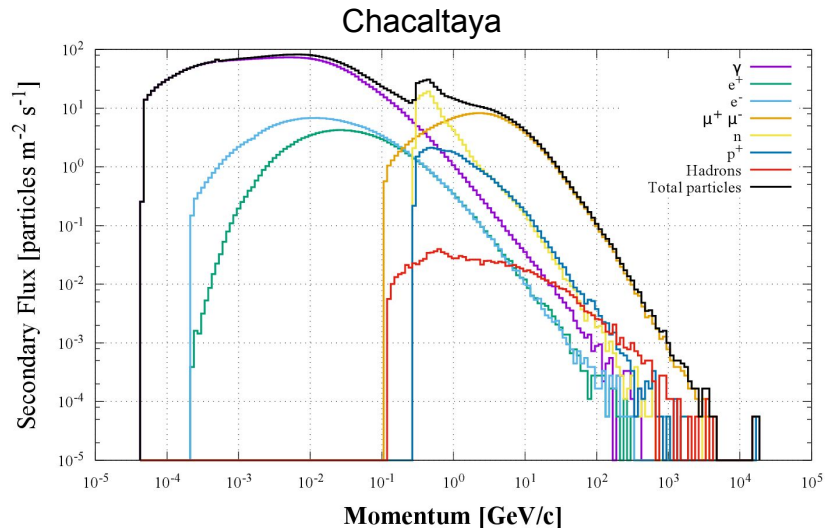


Figure 2: Spectrum of the secondary particles at two LAGO sites: Chacaltaya, Bolivia (5240 m a.s.l.) and La Serena, Chile (28 m a.s.l.). The comparison of the two graphics evidence a difference of one order of magnitude (at  $\sim 10^{-2}$  GeV/c) in the total of secondaries (black line).

LAGO site	Alt [m a.s.l.]	$\Xi^{\text{EM}}$ [m <sup>-2</sup> s <sup>-1</sup> ]	$\text{GE}^{\text{EM}}$ [%]	$\Xi^{\mu}$ [m <sup>-2</sup> s <sup>-1</sup> ]	$\text{GE}^{\mu}$ [%]	$\Xi^n$ [m <sup>-2</sup> s <sup>-1</sup> ]	$\text{GE}^n$ [%]	$\Xi^{\text{All}}$ [m <sup>-2</sup> s <sup>-1</sup> ]	$\text{GE}^{\text{All}}$ [%]
CHA	5240	4030	-15.4	231	-12.5	150	-81.3	4450	-17.7
LSC	28.00	282.0	-2.48	96.0	-1.04	4.00	-25.0	384.0	-2.60

## Cosmic Background Radiation at ground corrected by Geomagnetic Field

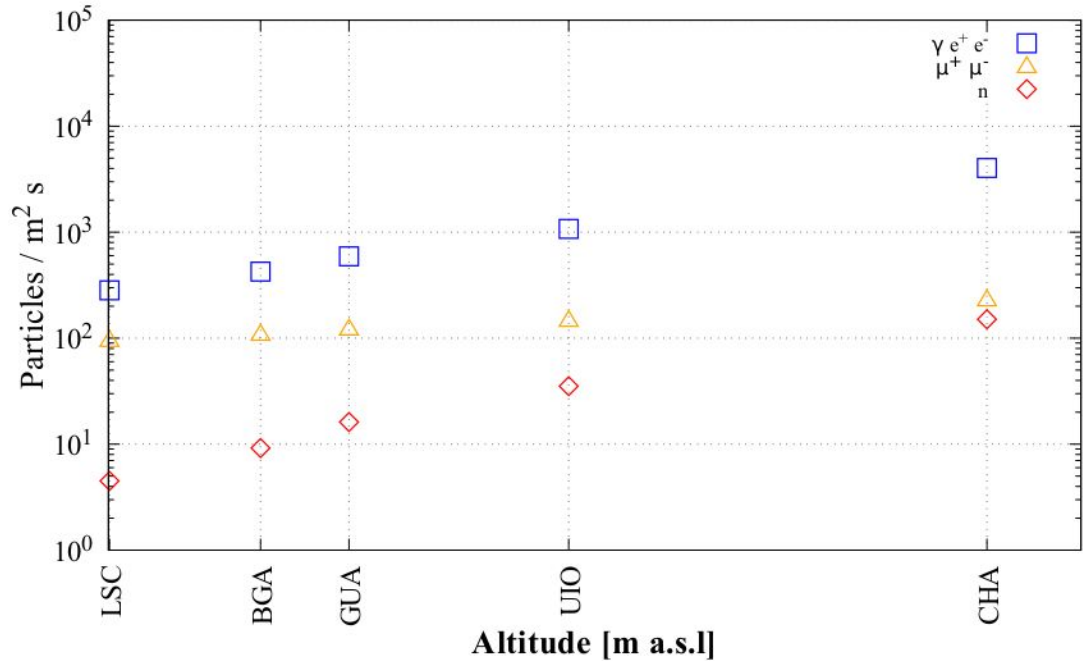
<b>LAGO site</b>	<b>Alt [m a.s.l.]</b>	$\Xi^{\text{EM}}$ [m <sup>-2</sup> s <sup>-1</sup> ]	$\text{GE}^{\text{EM}}$ [%]	$\Xi^{\mu}$ [m <sup>-2</sup> s <sup>-1</sup> ]	$\text{GE}^{\mu}$ [%]	$\Xi^{\text{n}}$ [m <sup>-2</sup> s <sup>-1</sup> ]	$\text{GE}^{\text{n}}$ [%]	$\Xi^{\text{All}}$ [m <sup>-2</sup> s <sup>-1</sup> ]	$\text{GE}^{\text{All}}$ [%]
CHA	5240	4030	-15.4	231	-12.5	150	-81.3	4450	-17.7
UIO	2800	1073	-9.87	147	-7.48	35.0	-60.0	1263	-11.6
GUA	1490	591.0	-3.72	123	-2.43	16.0	-31.2	733.0	-4.22
BGA	956.0	424.0	-5.42	109	-3.66	9.00	-44.4	544.0	-5.88
LSC	28.00	282.0	-2.48	96.0	-1.04	4.00	-25.0	384.0	-2.60

Table 1: Flux of cosmic background radiation at ground  $\Xi$  estimated at five LAGO sites: Chacaltaya, Bolivia (CHA); Quito, Ecuador (UIO); Ciudad de Guatemala (GUA); Bucaramanga, Colombia (BGA); and La Serena, Chile (LSC).

# Cosmic Background Radiation at ground corrected by Geomagnetic Field

Flux  $\Xi$  of cosmic background radiation at ground for each LAGO site and for the different components:  
electromagnetic in blue squares,  
muonic in yellow triangles and neutrons in red diamonds.

The flux  $\Xi$ , increases with the altitude as expected due to atmospheric absorption.





# The LAGO-GD: GEANT4 simulation to estimate the signal detected by the WCD to the flux of cosmic background radiation

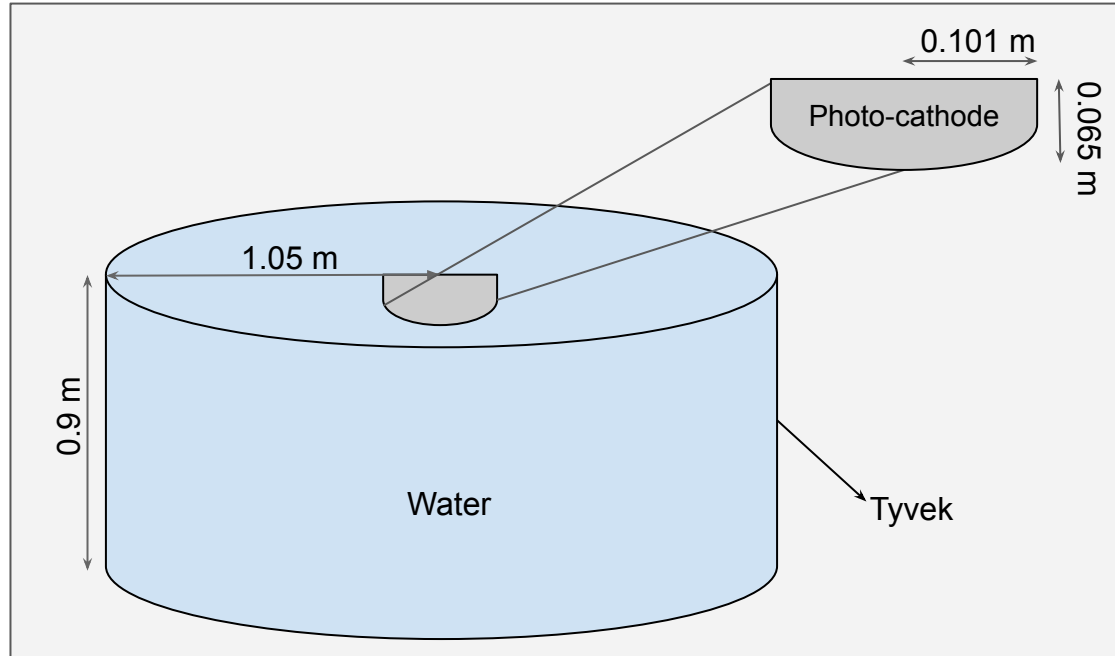


Figure 4. The standard LAGO WCD

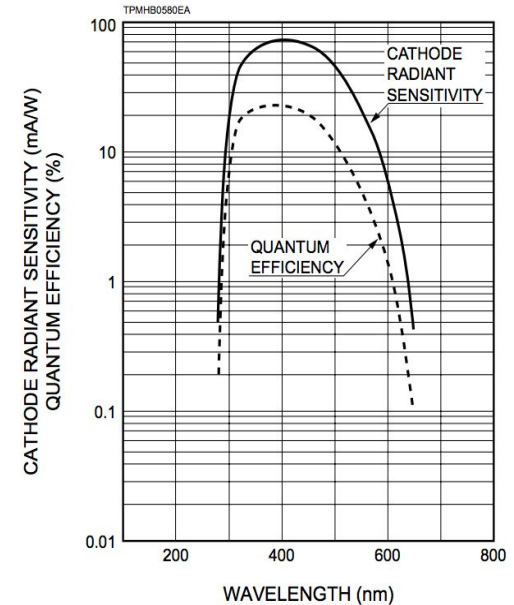


Figure 5. Quantum efficiency of the PMT R5912-Hamamatsu

## Estimation of the unit of calibration: VEM

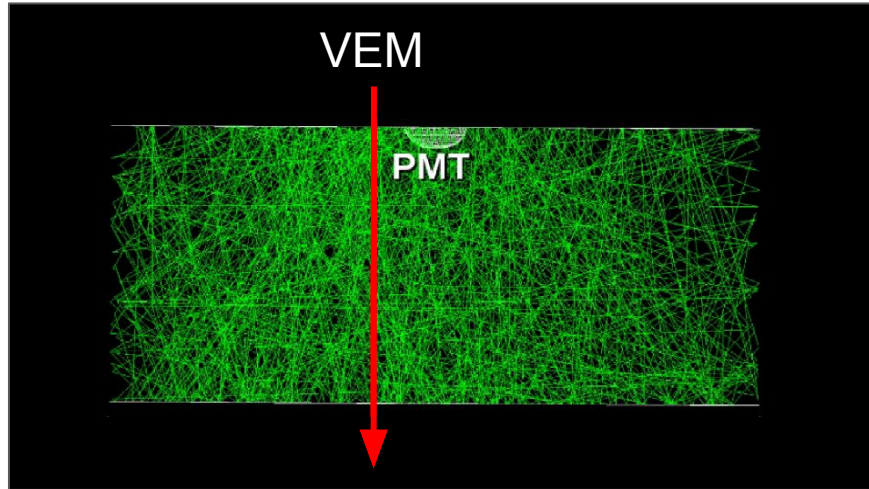


Figure 7. A vertical equivalent muon (VEM) crossing the standard WCD of LAGO.

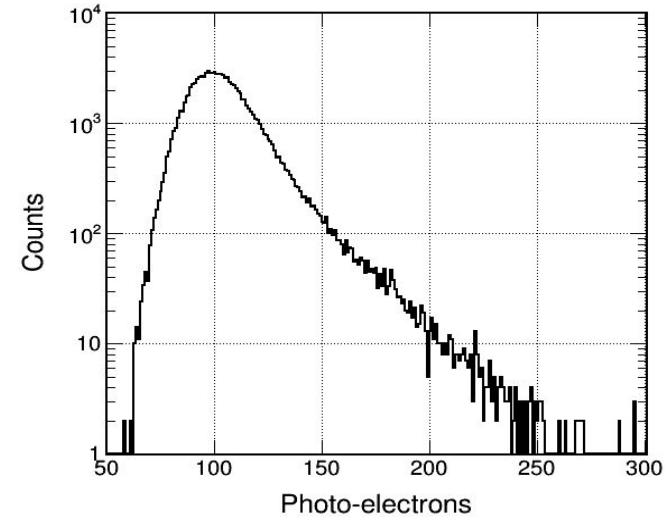


Figure 8. Distribution of the number of photo-electrons for  $10^5$  VEM of 3 GeV. The mode of **100 pe** represents the unit of calibration (1 VEM), that corresponds to **180 MeV** of energy deposited.

# Estimation of the signal detected by the LAGO's WCD to the flux of cosmic background radiation

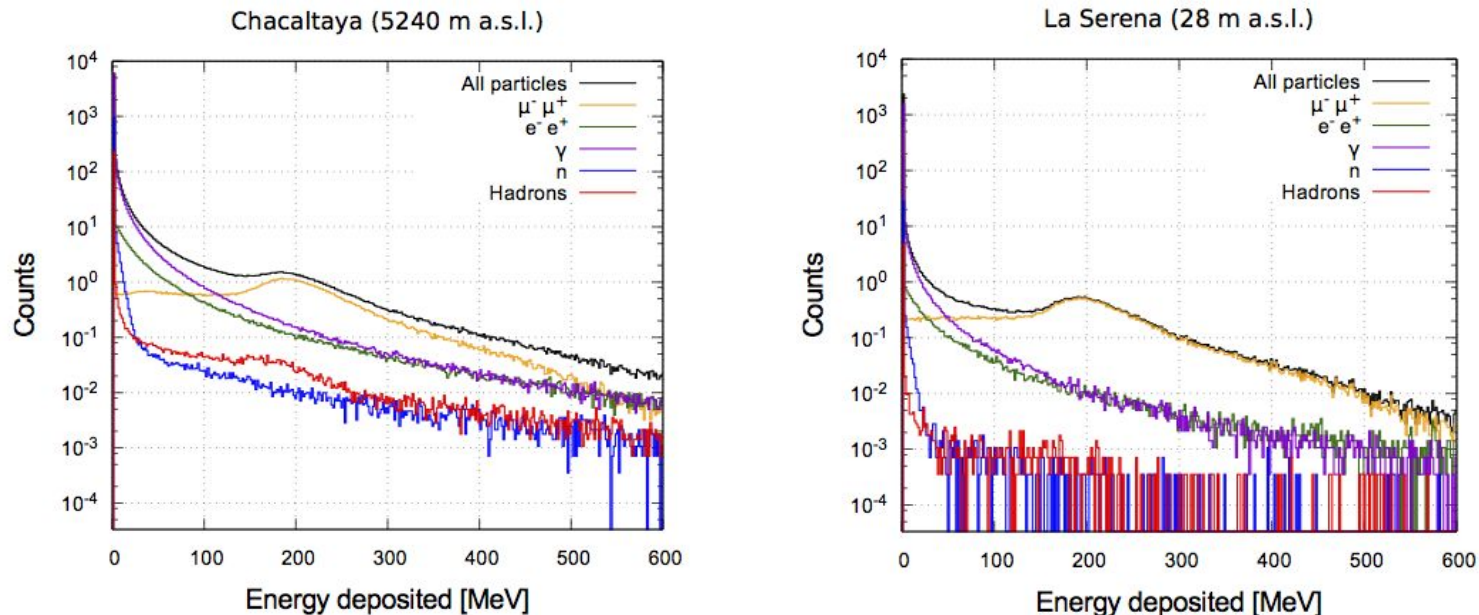


Figure 9: Charge histograms obtained for Chacaltaya (left) and La Serena (right). The black curves represent the total deposited energy and the colour ones represent the contribution of the EAS components.

**Rate of the secondary particles detected in the WCD for five LAGO sites, and the energy deposited by the electromagnetic component, muon component, neutrons, and all the particles.**

<b>LAGO Site</b>	$\Xi^D \times 10^3 [\text{m}^{-2} \text{s}^{-1}]$	$E^{\text{EM}} [\text{GeV}]$	$E^\mu [\text{GeV}]$	$E^n \times 10^{-1} [\text{GeV}]$	$E^{\text{All}} [\text{GeV}]$
CHA	1.80	1.49	0.22	0.49	1.77
UIO	0.52	0.40	0.14	0.11	0.55
GUA	0.31	0.22	0.11	0.05	0.34
BGA	0.23	0.16	0.10	0.03	0.26
LSC	0.17	0.11	0.09	0.01	0.20

## Discussions and remarks

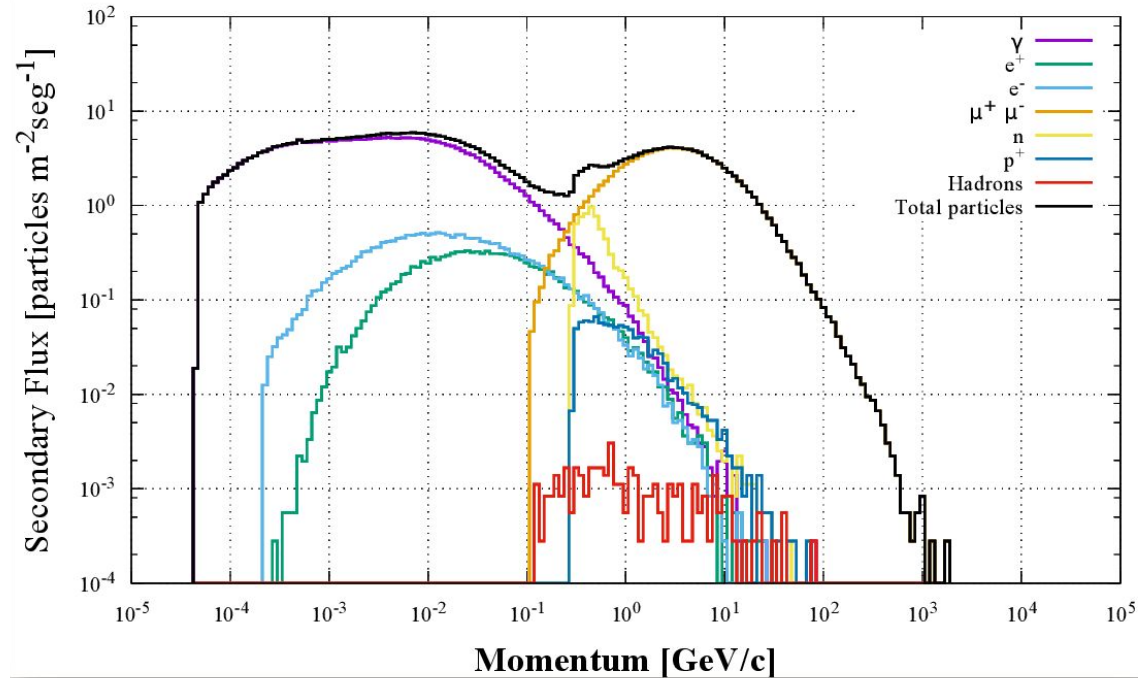
The ARTI framework, which we present here, allows us to estimate what would be the charge histogram for each site of LAGO. Therefore, those histograms can be compared with the data collected experimentally in order to calibrate the WCDs.

In addition, this work agrees with the results presented in where the relationship between the secondary particle flux and the height at which the detector is located was shown. Finally, we were able to develop a tool that estimates the flux of secondary particles detected by a WCD in any geographic position and at any time of the year.

**Thank you**

# Backup

## Marambio Antártida-Argentina (SAWB)



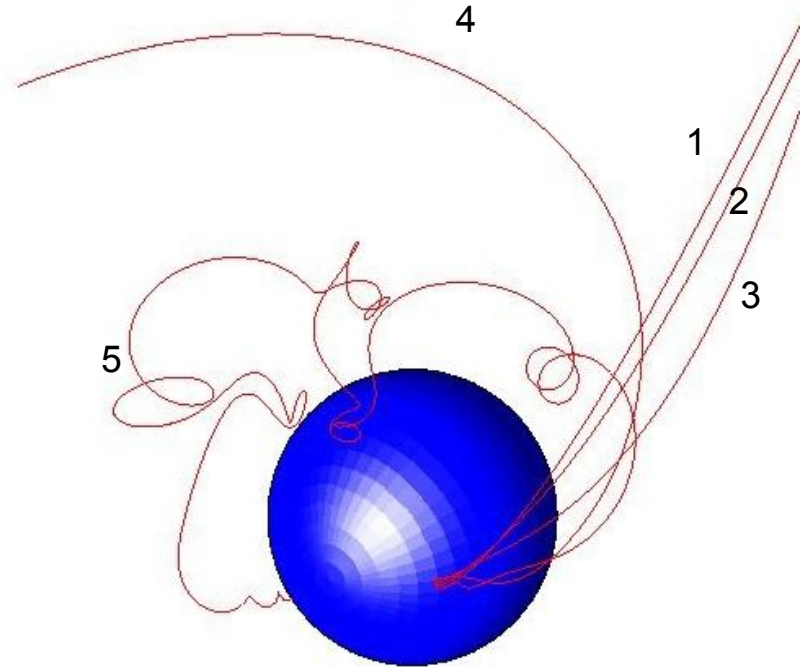
LAGO site	Alt [m a.s.l.]	$\Xi^{\text{EM}}$ [m <sup>-2</sup> s <sup>-1</sup> ]	$\text{GE}^{\text{EM}}$ [%]	$\Xi^{\mu}$ [m <sup>-2</sup> s <sup>-1</sup> ]	$\text{GE}^{\mu}$ [%]	$\Xi^n$ [m <sup>-2</sup> s <sup>-1</sup> ]	$\text{GE}^n$ [%]	$\Xi^{\text{All}}$ [m <sup>-2</sup> s <sup>-1</sup> ]	$\text{GE}^{\text{All}}$ [%]
SAWB	196.0	295.0	-0.33	108	-0.18	6.00	-6.15	411.0	-0.48



# Cosmic Background Radiation at ground corrected by Geomagnetic Field

This method builds a magnetic rigidity cutoff ( $R_c$ ) as a function of the geographical latitude, longitude, altitude above sea level, the arrival direction ( $\varphi$  and  $\theta$ ) and a cumulative probability distribution function.

- **CORSIKA** has correction of the geomagnetic field from height at sea level up to 112 km
- **MAGCOS** makes the correction from 112 km outside with the IGRF models (up to 5 ground radii) + Tsyganenko 2001 (more than 5 ground radii)



# The LAGO-GD: GEANT4 simulation to estimate the signal detected by the WCD to the flux of cosmic background radiation

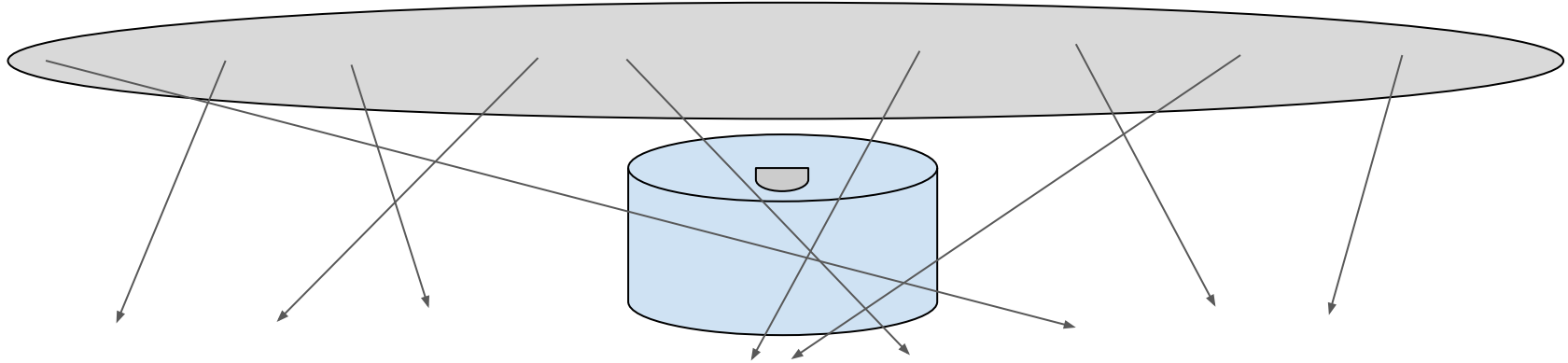


Figure 6. Distribution of the flux  $\Xi$  obtained with the LAGO-SW used as an input in the LAGO-GD to estimate the signal detected by the standard WCD of LAGO sites